# Mobilised Frictional Shear and Dead-Weight of Sand Wedge: Contributing to the Pull-Out Resistance of Belled Anchor Pile in Sand

Deb T. [1] and Pal S.K.. [2]

[1] Visiting Lecturer. Khumlwng Polytechnical collage, TTAADC Polytechnical Collage
`debtanaya88@gmail.com`
[2] Professor, Department of Civil Engineering, NIT Agartala, Tripura, 799046, India
`skpal1963gmail.com`

**Abstract.** This study explains the pull-out resistance of belled anchor pile under vertical tension, by using 1-g panel of belled anchor pile (2-D) possessing embedment ratios ($L/W_b$) of 3 to 5, thickness ratios ($W_s/W_b$) of 0.28 to 0.46, and bell angles ($\alpha$) of 45 to 72° in dyed and non-dyed dry sand deposit. Under vertical pull the applied stresses are acting along the vertical plane of the panel and so symmetrical non-linear slip surfaces are formed in both the sides of each panel. To predict pull-out resistances, the slip surfaces are interpreted as 3-D axisymmetric failure wedges surrounding the anchor models of same scale. The predicted pull-out resistance of each model is the combination of mobilised frictional shear and dead-weight of sand wedge. The values of pull-out resistance are within the range of 22.88 to 383.70 N. The pull-out resistances are increased with higher $L/D_b$, lesser $D_s/D_b$ and $\alpha$ of anchor models based on variation in the horizontal extent of failure points in slip surfaces. The ratios of mobilised frictional shear to pull-out resistance ($\times$ 100, %) of anchors are within the range of 13.50 to 30.81% and these values are decreased due to higher $L/D_b$ and, increased due to higher $D_s/D_b$ and $\alpha$. The ratios of dead-weight of sand wedge to pull-out resistance of anchors ($\times$ 100, %) are within the range of 69.20 to 86.50% and these values are increased due to higher $L/D_b$ and, decreased due to higher $D_s/D_b$ and $\alpha$.

**Keywords:** Pull-out resistance, belled anchor, slip surfaces, mobilised frictional shear, dead-weight of sand wedge.

## 1    Introduction

The scopes of anchor piles occupied a wide-space in foundation engineering applications in both off-shore and on-land structures. The anchor pile, whose enlarged base is making particular bell angle with the shaft, is known as belled anchor pile. A belled anchor pile may be specified by bell angle ($\alpha$), bell-diameter ($D_b$), shaft-diameter ($D_s$), embedment ratio ($L/D_b$) and diameter ratio ($D_s/D_b$). Depending upon the depth of embedment of the anchor in the soil and termination of failure surface either upto soil-surface or within soil mass, the anchor is classified either as a (a) shallow anchor and (b) deep anchor. For shallow anchor, failure pattern is general type that

reaches up to soil-surface in collapsed stage and failure occurs due to shear only; whereas, in case of deep anchor, the effect of soil-surface disappears.

In earlier days pull-out resistance was predicted by Majer's soil cone theory (1955) and Mors's earth pressure theory (1959). Turner (1962) disagreed the soil cone method as predicted pull-out resistance of deeper foundation was highly overestimated. The studies on linear mathematical models of sand wedge were carried out by Downs and Chieurzzi (1966), Clemence and Veesert (1977), Sutherland et al. (1882), Veermeer and Sutjiadi (1985), Murray and Geddes (1987) and Vanitha et al. (2007), where pull-out resistance was the summation of frictional resistance and dead-weight of sand wedge. Balla (1961) first introduced non-linear slip surface to predict pull-out resistance of anchor. The non-linear mathematical models of sand wedge were introduced by Matsuo (1967), Rao and Kumar (1987), Chattopadhyay and Pise (1986), Saeedy (1987) and Ghaly and Hanna (1994), where the anchor failure mechanism was controlled by combination of dead-weight of sand wedge surrounding anchor contributing in passive resistance and mobilised frictional shear along slip surface reverse to direction of wedge movement. Meyerhof and Adams (1968) suggested that pyramidal slip surface around the shallow anchor was initiated from the edge of anchor base and terminated in sand surface. Matsuo (1967), Dickin (1988), Tagaya et al. (1988), Dickin and Leung (1992), Ilamparuthi and Muthukrisnaiah (1999) and Ilamparuthi et al. (2002), Nazir et al. (2007) experimentally investigated the non-linear sand wedge around the shallow anchors from edge of anchor base to sand surface.

Though the present literature is providing a good number of mathematical models of sand-wedge to predict pull-out resistance, but there is a scarcity in the availability of data on the variation of mobolised frictional shear and dead-weight of sand wedge based on pull-out resistance in reference of embedment ratios ($L/D_b$), diameter ratios ($D_s/D_b$) and bell angles ($\alpha$).

## 2    Objective of the Study

A 1-g 2D belled anchor panel possessing a bell angle ($\alpha$), base diameter ($D_b$) and shaft diameter ($D_s$) is embedded in dyed and non-dyed dry sand deposits. Under vertical pull, as the applied stresses are acting along the vertical plane of the panel a couple of symmetric non-linear slip surfaces are formed in both the sides of each panel as shown in Fig.1. These slip surfaces are generated from the anchor-base and terminated in the sand surface. For the mathematical idealisation purpose, this slip surfaces can be interpreted as three-dimensional axisymmetric sand-wedges of the same scale. Each model is subjected to static upward pull i.e., $Q_{u.pred.}$, is the combination of as mobilised frictional shear and dead-weight of sand wedge.

The aim of the present study is to illustrate the (a) predicted values of pull-out resistance ($Q_{u.pred.}$) on the reference of horizontal extensions in slip surfaces, (b) ratio of mobilised frictional shear to pull-out resistance ($\times 100$, %) and (c) ratio of dead-weight

of sand wedge to pull-out resistance of belled anchors ($\times$ 100, %) on accounts of variation in embedment ratios, diameter ratios and bell angles in the dry sand deposit.
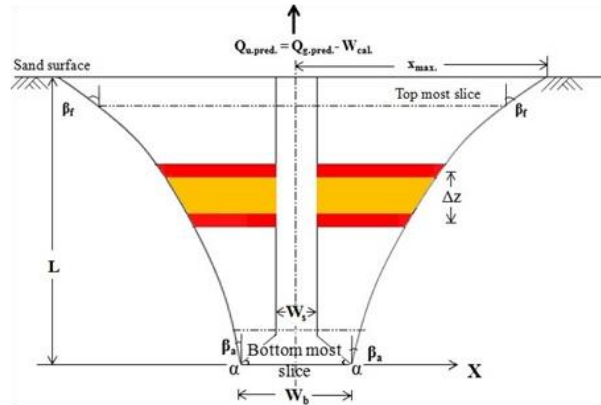


**Fig. 1.** A 1-g 2D belled anchor panel Under vertical pull in dyed and non-dyed dry sand deposits

## 3    Materials, Models, Testing-Tank and Sand Bed Preparation

The uniformly graded sand used in present study is procured from the local market. The preparation of foundation media with dry sand makes it easy to maintain the density of sand within the testing tank.  Fig. 2 shows grain size distribution curve of sand sample. The sand is having uniformity coefficient 1.1 and specific gravity 2.67. The maximum and minimum dry densities are found to be 14.20 and 16.50 kN/m$^3$ respectively. The placement density is fund to be 15.60 kN/m$^3$ at a certain calibrated height of free fall (700 mm) of sand by rainfall technique (Dash and Pise, 2003 and Dickin and Leung 1990). The angle of shearing resistance, i.e., $\phi$ = 33.5° at the placement density according to UU triaxial test.

1 mm thick mild steel plate is used to fabricate the 2-D panels. The length and height of each panel is 590±5 mm and 650 mm respectively. The thickness ($W_s$) of shaft part of the panel is 26 mm. The bell parts are having a range of thickness ($W_b$) as 92, 80, 68 and 56 mm and hence $W_s/W_b$ values are obtained as 0.28, 0.33, 0.38 and 0.46. All the panels are having bell angles ($\alpha$) of 45, 54, 63 and 72°. At the top of the panels a threaded small cylinder is welded to connect it to the proving ring (1 kN capacity) and pulling shaft gently. In that small cylinder two horizontally projected steel strips are provided to hold dial gauges (LC = 0.01 mm) on them and they are 180° apart from each other.

The testing-tank is 700 mm (Length) $\times$ 600 mm (Width) $\times$ 700 mm (depth). The wall of model tank is made of plaxiglass in four sides. Vertical steel stiffeners are provided in

three sides (except the front side) to prevent wall deflection outwards. To take uninterrupted measurements of failure points from outside no stiffeners are provided in front wall. A 12 mm thick plaxiglass in front-side is found to be stiffer enough to prevent outward wall deflection. The size of the tank is 6.5 times larger than the largest panel-base as concerned in the present test and so the tank size is large enough to avoid boundary effects.

To study the sand wedges, homogeneous sand media is prepared by placing successive layers of 3 mm thick red dyed and 18 mm thick non-dyed sand. The combination of dyed and non-dyed layer is chosen as well-suitable to prepare the foundation bed maintaining predetermined density of sand. The filling of testing-tank is continued by dyed and non-dyed sand layers until each panel attain embedment ratio ($L/W_b$) 3, 4 and 5. When the thickness of upper most layer is found to be less than 3 mm then it is adjusted along with the continuation of preceding layer (either dyed or non-dyed sand layer).

## 3.1 Experimental program

For those anchors, slip surfaces terminate up to sand surface at collapsed stage are known as shallow anchors (Krishnaswamy and Parashar 1994, Saran et al. 1986, and Vesic1969). Each panel is buried to attain embedment ratio ($L/W_b$) = 3, 4 and 5, the panels are having thickness ratio ($W_s/W_b$) = 0.46, 0.38, 0.33, and 0.28, and these are possessing bell angle ($\alpha$) = 45, 54, 63 and 72°. To carry out the study, total 48 numbers of experiments are performed to investigate the variations in lateral extension of slip surfaces in both the sides of panels buried in dry sand deposits.The values of $L/W_b$ and $W_s/W_b$ as mentioned for 2-D panel is exactly same used for the 3-D anchor models as $L/D_b$ and $D_s/D_b$ respectively.

## 3.2 Experimental set-up, test procedure and observations

The experiments performed as mentioned earlier are meant for the evaluation in the variations in the horizontal extension of failure points corresponding to the known vertical levels. Fig. 3 shows the schematic diagram of experimental set-up consisting of loading frame, panel installed inside the testing-tank, dyed and non-dyed sand layers, pulling shaft and attached proving ring with it, position and attachment of dial gauges and other accessories. The steel channels are used to fabricate the loading frame and the base is fixed with concrete-floor by bolt connection. A nut (along with ball-bearing arrangement), designed to rest on the reaction beam. A pulling shaft, is mechanically working on nut and screw motion. The pulling shaft is attached with panel through proving ring. Thus the panel is placed vertically at the centre of testing-tank on compacted sand bed. Upward vertical movement of shaft is operated by manually controlled circular rotating wheel. The wheel is connected with nut arrangement. Due to the clock-wise motion of wheel, the panel shifts upward graduaInitially prior to each test, a compacted sand bed of 100 mm thick is prepared

inside model tank over which the panel is placed. Each panel is subjected to vertical pull without causing any obliquity and tilt. The testing-tank is filled up with dyed and non-dyed sand layers to attain desired embedment depth. The pictorial view of slip surfaces as obtained from laboratory experiments presented in Figs. 4 (a and b) illustrate the formation of symmetric slip surfaces in both the sides of panels. The failure point at any horizontal level and vertical level can be distinguished by normal horizontal scaling from centre line of panel thickness to the failure point and by accounting the numbers dyed and non-dyed sand layers.
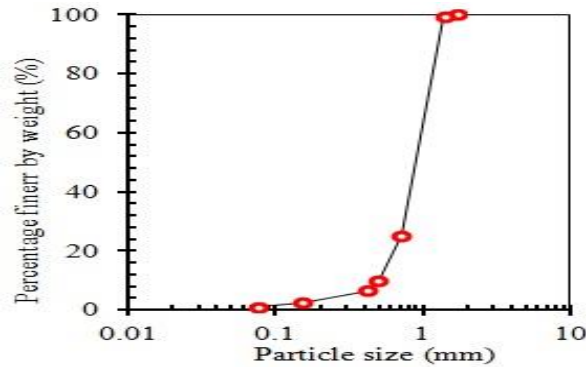


**Fig. 2.** Grain size distribution of sand samples

## 4 Model Identifications

Each model or panel is identified by a general coding form having four parts, which belong to bell angle, diameter ratio (or thickness ratio) and embedment ratio sequentially. For example, a 45° belled anchor panel possessing $W_s/W_b = 0.38$ at $L/W_b = 4$ is identified as 45-0.38-4. The symbol 72-0.28-3 represents a 72° panel, is possessing $W_s/W_b = 0.38$ and it is installed at $L/W_b = 3$.



1. *Pulling shaft*
2. *Nut*
3. *Rotating wheel*
4. *Ball-bearing system*
5. *Reaction frame*
6. *Proving ring*
7. *Dial gauges*
8. *Magnetic base*
9. *Magnetic base fixtures*
10. *Panel*
11. *Test tank*
12. *Sand bed*
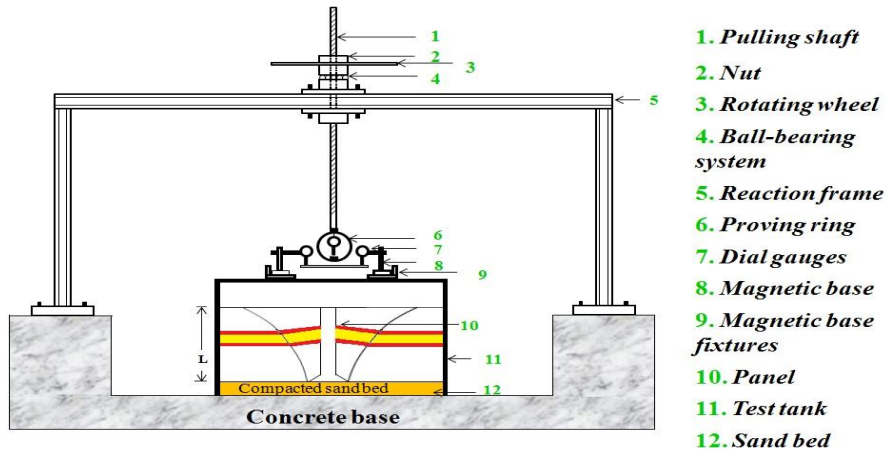
**Fig. 3.** Schematic view of the experimental set-up

## 5 Prediction of Pull-out resistance Based on Horizontal Slice Method

For the mathematical idealisation purpose and to calculate the pull-out resistance, the obtained slip surfaces are interpreted into axisymmetric three dimensional figure of same scale. The whole wedge is the integration of number of horizontal slices of known thickness ($\Delta z = 21$mm) as shown in Fig.5. The pull-out resistance of each slice is the summation of mobilised frictional shear on slip surface of slices opposite to the direction of anchor movement and dead-weight of sand wedge. The mathematical analysis is presented elsewhere in details (Deb and Pal, 2018).
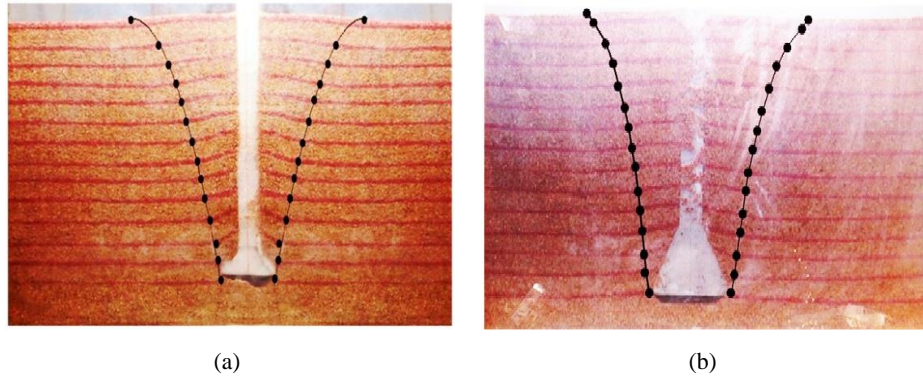


**Fig. 4.** Typical pictorial views of failure surface in both the sides of panels **(a)** 45-0.38-4 and **(b)** 63-0.28-3

Vertical component of shear resistance ($T_{vi}$) for $i^{th}$ slice surface,

$$T_{vi} = \left[ 2\gamma\pi\Delta Z \left( x_i + \frac{\Delta x_i}{2} \right) \{(Z_i + \Delta Z) - Z_i\} \{k_0 cos\beta_i + sin\beta_i\} tan\phi \right] \qquad \text{... (i)}$$

Dead-weight of $i^{th}$ slice,

$$W_{i.} = \left[ \pi\gamma \frac{\Delta Z}{3} \{x_i^2 + +(x_i + \Delta x_i)^2 + x_i(x_i + \Delta x_i)\} \right] \qquad \text{... (ii)}$$

Considering vertical equilibrium for all elementary forces, gross pull-out resistance of $i^{th}$ slice as follows:

$$Q_{i.g} = \left[ 2\gamma\pi\Delta Z \left( x_i + \frac{\Delta x_i}{2} \right) \{(Z_i + \Delta Z) - Z_i\} \{k_0 cos\beta_i + sin\beta_i\} tan\phi \right] + \left[ \pi\gamma \frac{\Delta Z}{3} \{x_i^2 + +(x_i + \Delta x_i)^2 + x_i(x_i + \Delta x_i)\} \right] \qquad \text{... (iii)}$$

Gross pull-out resistance for total wedge is found by summing up gross pull-out resistances for all the n number of slices,

$$Q_{g.pred.} = \sum_{i=1}^{n} Q_{i.g.pred.} \qquad \qquad \text{... (iv)}$$

Net or predicted pull-out resistance, $Q_{u.pred.} = Q_{g.pred.} - W_{cal.}$ \qquad ... (v)
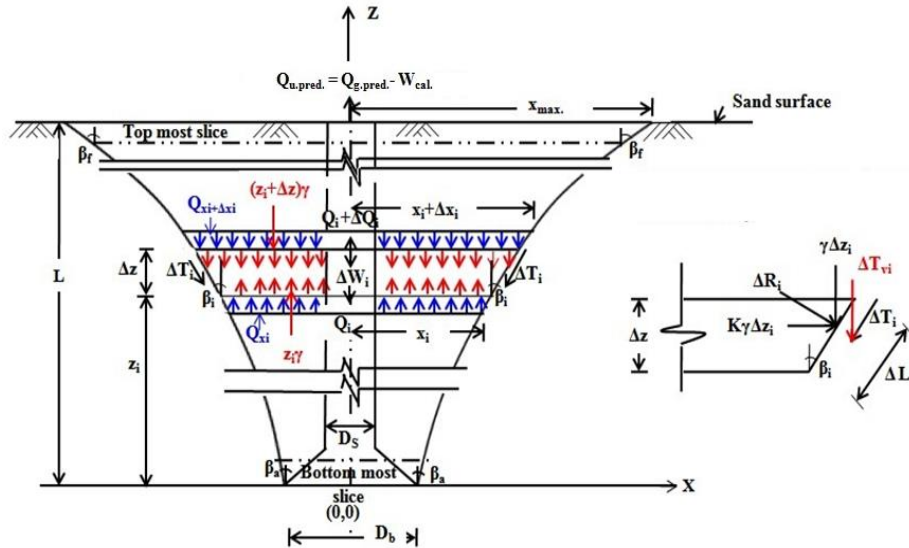


**Fig. 5.** Free body diagram of three dimensional $i^{th}$ slice wedge as per horizontal slice method

## 6 Results and Discussions

The effect of predicted pull-out resistances, ratio of mobilised frictional shear and dead-eight of sand wedge to the pull-out resistances are discussed based on the experimental observation on horizontal extension of failure points in slip surfaces of sand-wedge and the application of horizontal slice method on the mathematical model. The range of the predicted pull-out resistance of all the models is from 22.88 to 383.70 N. The values of ratio of mobilised frictional shear to the pull-out resistance ($\times 100,\%$) are from 13.50 to 30.81% and ratios of dead-eight of sand wedge to the pull-out resistance ($\times 100,\%$) are from 69.20 to 86.50%.

**6.1 Pull-out resistance, ratios of mobilised frictional shear and dead-weight of sand wedge based on pull-out resistance of belled anchor piles influenced by embedment ratios ($L/D_b$)**

In Fig. 6(a), the typical plots present the pull-out resistance vs. embedment ratio relationships for the models of $\alpha = 45$, 54 and 63° and having $D_s/D_b = 0.33$, 0.28 and 0.38 respectively. These figure signify that with the increase in the value of $L/D_b$ (i.e., 3, 4 and 5), the same belled anchor pile can achieve higher pull-out resistance and this

trend is true regardless the values of $D_s/D_b$ and $\beta$. For higher $L/D_b$ values, with higher anchor installation depth, gradually larger overburden pressure would act on the anchor base. As a result, gradually larger sand wedges are formed and offer higher pull-out resistances, as shown in Fig. 6(b) besides panel 45-0.33 at $L/T_b$ = 3, 4 and 5. A similar pattern in the relationship of pull-out resistance with embedment ratio was also established by Dickin and Leung (1990), Ghosh and Bera (2014), Bera (2014), and Nazir et al. (2014) in dry sand bed.

The typical Fig. 7(a) illustrates that the ratio of mobilised fictional shear to pull-out resistance ($\times$ 100, %) values gradually decrease with higher values of embedment ratio for all the 45° models. The typical Fig. 7(b) presents that for the same models, the ratio of dead-weight of sand wedge to pull-out resistance ($\times$ 100, %) values gradually increase with higher values of embedment ratio. This is due to the reason that for the sand wedges around the 45° model of $D_s/D_b$ = 0.33, at $L/D_b$ = 3, 4 and 5, the values of mobilised fictional shear is only 22.26, 18.84 and 16.76% of the pull-out resistance respectively. Whereas, for this model and similar embedment depths the
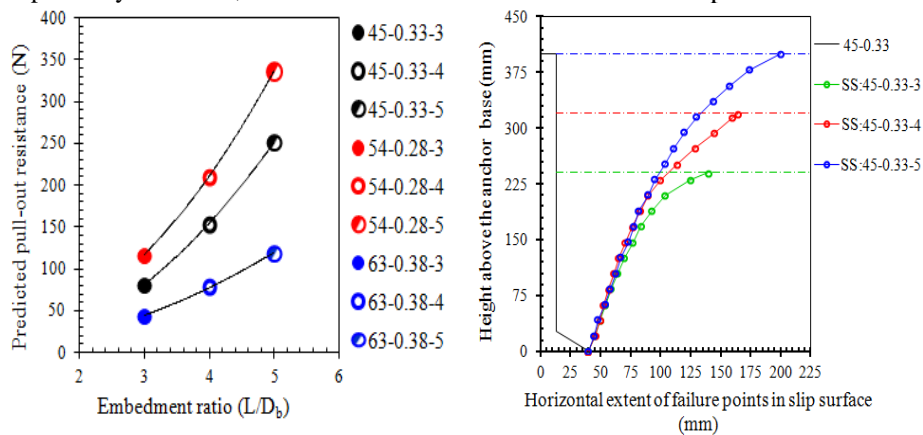


**Fig. 6. (a)** Predicted pull-out resistance vs. embedment ratio relationships for 45, 54 and 63° belled anchor pile model and having corresponding $D_s/D_b$ = 0.33, 0.28 and 0.38

**Fig. 6. (b)** Height above the anchor base vs. horizontal extent of failure points in slip surface relationship besides panel 45-0.33 at $L/T_b$ = 3, 4 and 5

dead-weight of sand wedge is 77.74, 81.16 and 83.24% of the pull-out resistance. The values of mobilised frictional shear, dead-weight of sand wedge and pull-out resistance increase with the formation of larger sand-wedges at deeper embedment depths. For the primary and secondary increments in pull-out resistances 91.41 and 62.24%, the rise in dead-weight of sand wedge are 96.47 and 65.14% and in mobilised fictional shear are 62.54 and 44.36% respectively. This represents that for the rise in pull-out resistance the contribution of dead-weight of sand wedge is more significant than the part of mobilised fictional shear.

(a)                                    (b)
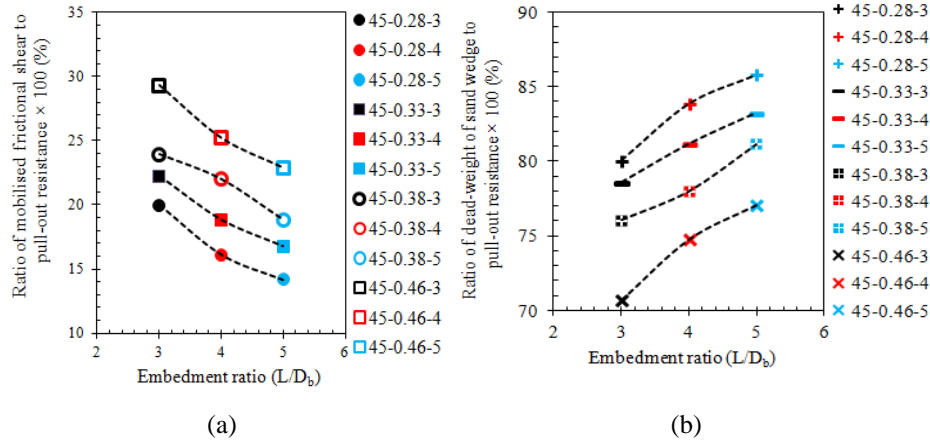
**Fig. 7.** The relationships of **(a)** ratio of mobilised frictional shear to pull-out resistance (×100, %) vs. embedment ratio and **(b)** ratio of dead-weight of sand wedge to pull-out resistance (×100, %)  vs. embedment ratio (×100, %), for all the models of 45°, having $D_s/D_b$ = 0.28, 0.33, 0.38 and 0.46

## 7.2    Pull-out resistance, ratios of mobilised frictional shear and dead-weight of sand wedge based on pull-out resistance of belled anchor piles influenced by diameter ratios ($D_s/D_b$)

In Fig. 8 (a), the typical plots present the pull-our resistance vs. diameter ratio relationships for the models of α = 63, 72 and 45° at $L/D_b$ of 4, 5 and 3 respectively. From the figure it can be noticed that as the anchors are possessing gradually higher values of $D_s/D_b$, i.e., from 0.28 to 0.33, from 0.33 to 0.38 and from 0.38 to 0.46 the pull-out resistance gradually decrease irrespective of α and $L/D_b$ values. In case of a particular $L/D_b$ value, for gradually higher diameter ratio lower overburden pressure act on anchor base; consequently smaller sand wedges are generated. The Fig. 8(b) reveals that the pull-out resistance are gradually lesser for 72-0.28-5, 72-0.33-5, 72-0.38-5 and 72-0.46-5. With a gradual increase in diameter ratio a decreasing pattern of pull-out resistance was also observed by Dickin and Leung (1990).

The typical Fig. 9(a) illustrates that the ratio of mobilised frictional shear to pull-out resistance (× 100, %) values gradually increase with higher values of diameter ratios for all the 63° models. The typical Fig. 9(b) reveals that for the same models, the ratio of dead-weight of sand wedge to pull-out resistance (× 100, %) values gradually decrease with higher values of diameter ratios. At the certain $L/D_b$ value, for the models having higher diameter ratios at shallow depth, gradually smaller sand wedges are formed on gradually smaller anchor bases. The values of mobilised frictional shear, dead-weight of sand wedge and pull-out resistance decrease with the formation of smaller sand-wedges at shallow embedment depth (but at same $L/D_b$). In the Fig. 9(b), for 63-0.28-4, 63-0.33-4, 63-0.38-4 and 63-0.46-4 the values of corresponding

mobilised frictional shear are only 16.66, 20.36, 22.74 and 26.07% and the respective values of dead-weight of sand wedge are 83.34, 79.64, 77.26 and 73.93% of pull-out
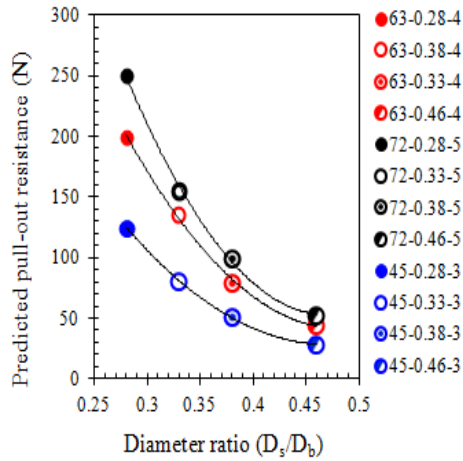


**Fig. 8(a).** Predicted pull-out resistance vs. diameter ratio relationships for 63, 72 and 45° belled anchor models and at corresponding $L/D_b = 4$, 5 and 3
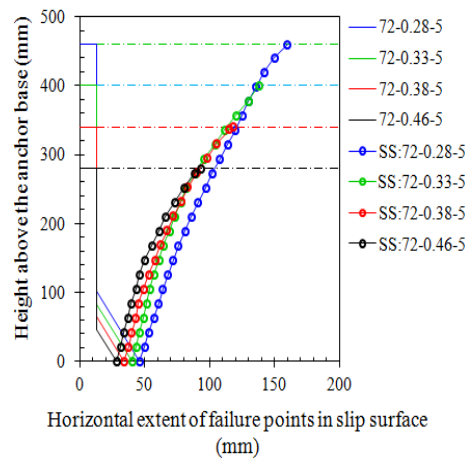
**Fig. 8(b).** Height above the anchor base vs. horizontal extent of failure points in slip surface relationships besides 72° panel at $L/T_b = 5$ and these are possessing $T_s/T_b = 0.28$, 0.33, 0.38 and 0.46

resistance. The decrements in pull-out resistances from model 63-0.33-4 to 63-0.28-4, from 63-0.33-4 to 63-0.38-4 and from 63-0.38-4 to 63-0.46-4 are 31.76%, 41.9% and 47.74%, whereas, the corresponding rise in mobilised frictional shear are 19.91%, 54.16% and, 66.85% and the decrease in respective dead-weight of sand wedge are 34.52%, 42.99% and 48.91% based on pull-out resistance. This statistical analysis represents that the involvement of dead-weight of sand wedge to pull-out resistance value is significantly large than the mobilised frictional shear values, so these two factors (in %) show reverse trend to each other.
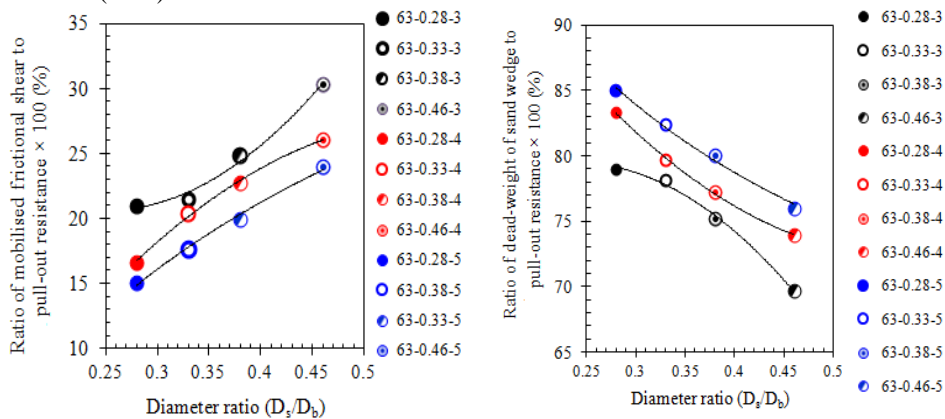


**Fig.9.** The relationship of (a) ratio of mobilised frictional shear to pull-out resistance vs. diameter ratio (×100, %) and (b) ratio of dead-weight of sand wedge to pull-out resistance vs. diameter ratio (×100, %), for all the models of 63°, installed at $L/D_b = 3$, 4 and 5

**7.3    Pull-out resistance, ratios of mobilised frictional shear and dead-weight of sand wedge based on pull-out resistance of belled anchor piles influenced by bell angles (α)**

In Fig. 10(a), the typical plots present the pull-out resistance vs. bell angle relationships for the models of $D_s/D_b$ = 0.33, 0.38 and 0.46 and at $L/D_b$ = 4, 3 and 5 respectively.  Form the figure it can be noticed that as the anchors are possessing gradually higher values of α, i.e., from 45 to 54°, from 54 to 63° and from 63 to 72°, pull-out resistances attain gradually decreasing pattern irrespective of $L/D_b$ and $D_s/D_b$ values.  At a particular embedment depth, for a certain $D_s/D_b$ value, in 72° anchors the slant height of bell is significantly steeper, so under vertical tension the influence zone above these anchor bases are very close to the anchor shaft; whereas, the slant height of bell for 45, 54 and 63° anchors are much milder than that of 72° anchor, so the influence zone above these anchors base are horizontally extended reasonably far away surrounding the anchor shaft. So, the models having higher bell angles form gradually smaller sand wedges; though the wedges for 45, 54 and 63° are very close to each other but wedges for 72° are reasonably smaller than other wedges as shown in Fig. 10(b), for panels possessing $T_s/T_b$ = 0.33 at $L/T_b$ = 4. So, the values of pull-out resistance decrease with the formation of smaller sand wedges. A similar failure trend was explained by Matsuo (1967). In this figure, for anchors having $D_s/D_b$ = 0.33, $L/D_b$ of 4 and α values from 45 to 54°, 45 to 63° and 45 to 72°, pull-out resistance values are decreased 3.24, 8.92 and 27.70%. In general, all the 63° belled anchors are within 10% less than 45° anchors, whereas, 72° belled anchors are within 30% less than 45° anchors. So, 45, 54 and 63° anchors are found to be more efficient as a tension resistant structure than 72° anchors. A similar trend in pull-out resistance was also noticed by Nazir et al. (2014) for anchors of bell angles 30 to 60° and Dickin and Leung (1992) for anchors of bell angles 22° to 72° in dry sand.
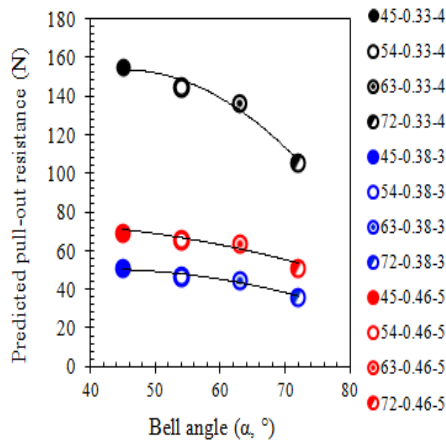


**Fig. 10(a).**    Predicted pull-out resistance vs. bell angle relationships for belled anchor models having $D_s/D_b$ = 0.33, 0.38 and 0.46 and at corresponding $L/D_b$ = 4, 5 and 3
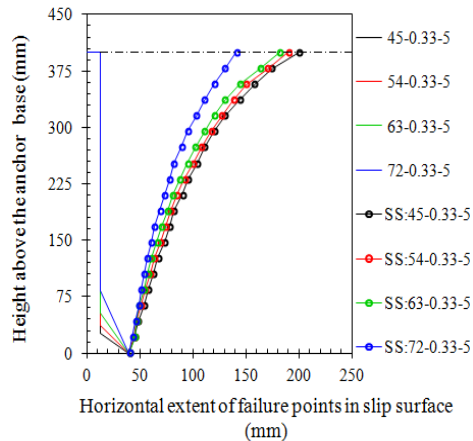
**Fig. 10(b)**.  Height above the anchor base vs. horizontal extent of failure points in slip surface relationships besides panels possessing $T_s/T_b$ = 0.33 at $L/T_b$ = 4 and these having α = 45, 54, 63 and 72°

The typical Fig. 11(a) illustrates that the ratio of mobilised frictional shear to pull-out resistance ($\times$ 100, %) values gradually increase with higher values of bell angles, i.e., 45, 54, 63 and 72°, for all the models of $D_s/D_b = 0.33$ and a certain series of $L/D_b = 3$, 4 and 5. For the same models, the typical Fig. 11(b) illustrates that the ratio of dead-weight of sand wedge to pull-out resistance ($\times$ 100, %) values gradually decrease with higher values of bell angle. In the Fig. 11(a and b), for 45-0.33-5, 54-0.33-5, 63-0.33-5 and 72-0.33-5 the values of corresponding mobilised frictional shear are only 16.76, 16.98, 17.64 and 18.75% and the respective values of dead-weight of sand wedge are 83.24, 83.02, 82.36 and 81.25 % of pull-out resistance. The decrements in pull-out resistances from model 45-0.33-5 to 54-0.33-5, from 45-0.33-5 to 63-0.33-5 and from 45-0.33-5 to 72-0.33-5 are 6.48, 9.19 and 28%, whereas, the corresponding rise in mobilised frictional shear are 1.31%, 5.25% and, 11.87% and the decrease in respective dead-weight of sand wedge are 0.26%, 1.06% and 2.4% based on pull-out resistance. This statistical analysis represents that due to the major contribution of dead-weight of sand wedge than the mobilised frictional shear values to acquire pull-out resistance, the trend of two ratios ($\times$100, %) in reference to bell angles are differing each other.
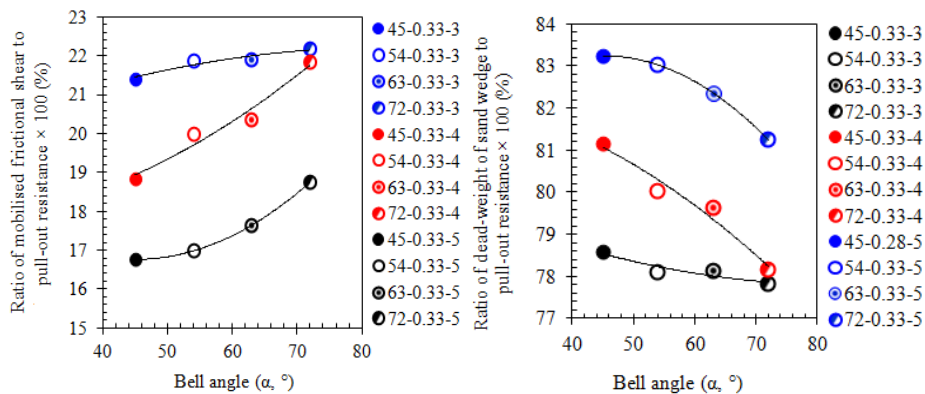


**Fig.11.** The relationships of **(a)** ratio of mobilised frictional shear to pull-out resistance vs. bell angle ($\times$100, %) and **(b)** ratio of dead-weight of sand wedge to pull-out resistance vs. bell angle ($\times$100, %), for all the models of having $D_s/D_b = 0.33$ and at $L/D_b = 3$, 4 and 5

## 7     Conclusions

The following significant conclusions may be drawn as listed below:
1. The variations in the horizontal extent of slip surfaces based on embedment ratios, thickness ratios and bell angles of 2-D panels lead to the variations in predicted pull-out resistance in 3-D models. The range of the predicted pull-out resistances of all the models are from 22.88 to 383.70 N.
2. The predicted pull-out resistances are increased with higher embedment ratios, lesser diameter ratios and bell angles.
3. The value**s** of ratio of mobilised frictional shear to the pull-out resistance

($\times 100,\%$) are from 13.50 to 30.81% .

4. The values of ratio of dead-eight of sand wedge to the pull-out resistance ($\times 100,\%$) are from 69.20 to 86.50%.

5. The ratios of mobilised frictional shear to pull-out resistance ($\times$ 100, %) of anchors are decreased and ratios of dead-weight of sand wedge to pull-out resistance of anchors ($\times$ 100, %) are increased due to higher embedment ratios. Whereas, the ratios of mobilised frictional shear to pull-out resistance ($\times$ 100, %) of anchors are increased and ratios of dead-weight of sand wedge to pull-out resistance of anchors ($\times$ 100, %) are decreased for higher values of diameter ratio and bell angle.

# References

1. Balla, A., The resistance to breaking-out of mushroom foundations for pylons, Proceedings of 5th International Conference on Soil Mechanics and Foundation Engineering. 1:569-576, Paris, (1961).

2. Bera, A. K., Parametric study on uplift capacity of anchor with tie in sand, Korean Society of Civil Engineers, 18(4):1028-1035 (2014).

3. Chottapadhyay, B.C., and Pise, P.J., Breakout resistance of horizontal anchors insand, Japanese Society of Soil Mechanics and Foundation Engineering. 26:126, 1986

4. Clemence, S.P., and Veesaert, C.J., Dynamic uplift resistance of anchors in sand, Proceedings of the International Conference on Soil-Structure Interaction, pp: 389-397, Roorkee, India, 1977.

5. Dash and Pise, " Effect of compressive load on uplift capacity of model piles," v. 129(11):987-992, (2003).

6. Dickin, E.A., Uplift behavior of horizontal anchor plates in sand, Journal of Geotechnical Engineering, 114 (11):1300-1317 (1988).

7. Dickin, E.A., and Leung, C.F., Performance of piles with enlarged bases subjected to uplift forces, Canadian Geotechnical Journal. 27:546- 556 (1990).

8. Dickin, E. A., and Leung, C.F., The influence of foundation geometry on uplift behaviour of piles with enlarged bases, Canadian Geotechnical Journal. 29:498-505 (1992).

9. Downs, D. I., and Chieurzzr, I. (1966). "Transmission tower foundations." ASCE Journal of the Power Division, v. 92, P02, pp. 91-114.

10. Ghaly, A., and Hanna, A., Ultimate uplift resistance of single vertical anchors. Canadian Geotechnical Journal. 31:666-672 (1994).

11. Ghosh, A., and Bera, A. K., Effect of geotextile ties on uplift capacity of anchors embedded in sand, Geotechnical Geology Engineering. 28:567-577(2010).

12. Ilamparuthi, K. and Muthukrishnaiah, K., "Anchors in sand bed: delineation of rupture surface," Ocean Engineering, v. 26, pp. 1249 − 1273 (1999).

13 .Ilamparuthi, K., Dickin, E. A. and Muthukrisnaiah, K., "Experimental investigation of the uplift behavior of circular plate anchors embedded in sand," Canadian Geotechnical Journal, v. 39, pp.648 – 664 (2002).

14. Krishnaswamy, N.R., and Parashar, S.P., Uplift behaviour of plate anchors with geosynthetics, Geotextiles and Geomembranes. 13.67-89 (1994).

15 .Matsuo, M., "Study of uplift resistance of footing (I)," Soil and Foundation. 7(4):1-37, (1967).

16. Majer, J., Zur Berechnung Von Zugfundamenten. Osterreichische Bauzeitschrift 10, H.5 (1955).

17. Mors, H., "The behaviour of mast foundations subject to tensile forces." Bautechnik 10, pp. 367-378 (1959).

18. Murray, E.J., and Geddes, J.D., "Uplift of anchor plates in sand," Journal of Geotechnical Engineering, 113(3):202-215 (1987).

19. Nazir. R., Moayedi. H., Pratikso. A., and Mosallanezhad, M., "The uplift load capacity of an enlarged base pier embedded in dry sand," Arabian Journal of Geosciences, v.8, pp 7285–7296.DOI 10.1007/s12517-014-1721-3 (2015).

20. Rao, K.S.S., and Kumar, J., Vertical uplift capacity of Horizontal anchors, Journal of Geotechnical Engineering. 120 (7):1134- 1147 (1994).

21. Saeedy, H.S., Stability of circular vertical earth anchors, Canadian Geotechnical Journal, 24:452-456 (1987).

22. Saran, S., Ranjan, G., Nene, A.S., Soil anchors and constitutive laws, Journal of Geotechnical Engineering, 112(12):1084-1100, 1986.

23. Sutherland, H. B. "Uplift resistance of soils," Geotechnique, v. 138, pp. 493 − 516 (1988).

Tagaya, K., Scott, R. F., and Aboshi, H., "Pull-out resistance of buried anchors in sand," Soils and Foundations, v. 28, pp. 114 − 130 (1988).

24. Turner, E. A., "Uplift resistance of transmission tower footings." Journal of Power Division, , v.88, pp. 17-32 (1962).

25. Vanitha, L., Patra, N.R., and Chandra, S., Uplift capacity of pile group anchors, Geotechnical Geological Engineering, 25:339- 347 (2007).

26. Vesic, A.S., Breakout resistance of objects embedded in ocean bottom, Soil Mechanics and Foundation., Report Number CR.69.031 prepared for U. S. Naval Civil Engineering Laboratory Port Hueneme, California under. Contract No. N6 2399-68-C-0043, 1969.

27. Vermeer, P. A., and Sutjiadi, W.. "The uplift resistance of shallow embedded anchors." Proceedings, 11th International Conference on Soil Mechanics and Foundation Engineering, San Francisco, CA, v. 4, pp.1635-1638 (1985).